IL NUOVO CIMENTO **38 C** (2015) 74
DOI 10.1393/ncc/i2015-15074-5

COMMUNICATIONS: SIF Congress 2014

Atomic and molecular far-infrared lines from high redshift galaxies

L. VALLINI

Dipartimento di Fisica e Astronomia, Università di Bologna, viale Berti Pichat 6/2, 40127 Bologna, Italy

received 30 January 2015

Summary. — The advent of Atacama Large Millimeter-submillimeter Array (ALMA), with its unprecedented sensitivity, makes it possible the detection of far-infrared (FIR) metal cooling and molecular lines from the first galaxies that formed after the Big Bang. These lines represent a powerful tool to shed light on the physical properties of the interstellar medium (ISM) in high-redshift sources. In what follows we show the potential of a physically motivated theoretical approach that we developed to predict the ISM properties of high redshift galaxies. The model allows to infer, as a function of the metallicity, the luminosities of various FIR lines observable with ALMA. It is based on high resolution cosmological simulations of star-forming galaxies at the end of the Epoch of Reionization ($z \simeq 6$), further implemented with sub-grid physics describing the cooling and the heating processes that take place in the neutral diffuse ISM. Finally we show how a different approach based on semi-analytical calculations can allow to predict the CO flux function at $z > 6$.

PACS 98.54Kt – Primordial galaxies.
PACS 98.58Bz – Atomic, molecular, chemical, and grain processes.
PACS 98.58Db – Molecular clouds.

1. – Introduction

Starting from the '90s of the XXth century, the number of high redshift observations has known a vigorous growth thanks to the usage of increasingly sensitive telescopes and sophisticated selection techniques [1].

The high sensitivity of state-of-the-art instruments such as the Hubble Space Telescope (HST), the Very Large Telescope (VLT), the Keck and Subaru telescopes combined with observational strategies such as the Lyman Break (*e.g.* [2-5]) and Lyman Alpha selection (*e.g.* [6-9]), allows to discover thousands of galaxies at $z > 5$ named Lyman Break Galaxies (LBGs), and Lyman Alpha Emitters (LAEs), respectively.

However, even though the Lyman Break and Lyα selection methods have been proved to be very successful techniques in finding high-z galaxies, they have also several drawbacks. For instance, approaching $z \approx 7$, the detections of LAEs via narrow-band imaging

become increasingly difficult due to the declining sensitivity of the detectors at $\approx 1\,\mu$m combined with the larger neutral hydrogen fraction in the intergalactic medium that causes an increase in the resonant scattering of the Lyα photons. Moreover, the characterization of fundamental galaxy properties (such as the star formation rate and the stellar mass) with the sole detection of the redshifted Lyα line and/or FUV continuum is extremely hard because they are strongly affected by dust extinction. Without a proper correction, the Lyα (or the UV continuum) can provide only lower limits on the SFR [10]. Hence, the detection of other lines beside the Lyα is a fundamental step toward the constraining of the ISM properties, the SFR, and the mass of the dust in high-z galaxies.

The far-infrared (FIR) atomic and molecular lines, and the dust continuum emission are the most suitable tracers to achieve this goal. From high-z, they are redshifted within the sub-millimeter/millimeter bands of the Atacama Large Millmeter/submillimeter Array (ALMA), the most powerful sub-millimeter interferometer on the Earth. The FIR atomic lines (mainly fine structure transition of C, N, O) trace the neutral/ionized gas and provide information about the thermodynamical and chemical properties of the gas. The strongest one is the $^2P_{3/2} \rightarrow ^2 P_{1/2}$ transition of the ionized carbon ([CII]) at $158\,\mu$m [11]. [CII] is the dominant coolant of the interstellar medium arising various environments such as the neutral diffuse gas in the ISM and the Photo Dissociation Regions. Nitrogen and oxygen lines ([NII], [OI] and [OIII]), despite their lower luminosity, are fundamental to constrain the metallicity and the strength of the radiation field within the galaxies and have been detected in several sources at $z > 4$ (*e.g.* [12-16]). Moreover, *molecular* FIR lines such as the CO rotational transitions are unique tracers of the cold gas that fuels the star formation. Finally, FIR lines, being completely unaffected by the dust extinction or resonant scattering such as the Lyα, are superb redshift estimators.

Before the ALMA advent, atomic/molecular lines and continuum from high-z have been studied using the Plateau de Bure Interferometer or the CARMA observatory. Despite the great capabilities of these interferometers, only extreme sources such as quasar hosts or sub-millimeter galaxies, characterized by star formation rates of the order of $\approx 1000\,M_\odot\,\mathrm{yr}^{-1}$ have been detected at $z > 4$ through metal cooling lines or dust continuum emission: [17-21]. ALMA makes it possible to carry out the search also in normal (*i.e.* SFR < 100) galaxies around the Epoch of Reionization. At the date of this publication, a handful of galaxies at $z \approx 4$–5 with modest star formation rates ($50 - 300\,M_\odot\,\mathrm{yr}^{-1}$) have been detected in [CII] or in continuum [22-25] but any observation has been reported yet in normal galaxy at $z \approx 7$ [26-28].

By making use of a zoomed cosmological simulation and of a sub-grid model describing the thermodynamical equilibrium of the neutral diffuse gas, we present detailed predictions for the intensity of several FIR emission lines ([CII] $158\,\mu$m, [OI] $63\,\mu$m) arising from th ISM a $z = 6.6$ galaxy. Moreover we show how we estimate the H_2 mass and the CO (6-5) line luminosity in a sample of $z \approx (5.7, 6.6)$ simulated LAEs.

2. – Numerical simulations

In what follows, we briefly introduce the numerical simulation and the sub-grid model developed to describe the thermal equilibrium of the neutral gas in the ISM. However, we defer the interested reader to [29] for an extended discussion about these arguments. We run cosmological SPH hydrodynamic simulations using `GADGET-2` [30]. We simulate a $(10h^{-1}\,\mathrm{Mpc})^3$ comoving volume with 2×512^3 baryonic + dark matter particles, giving a mass resolution of $1.32\ (6.68)\times10^5\,M_\odot$ for baryons (dark matter). We select a snapshot at redshift $z = 6.6$, and we identify the most massive halo (total mass $M_h = 1.17\times10^{11}\,M_\odot$)

by using a Friend-of-Friend algorithm. We select a $(0.625\,h^{-1}\,\mathrm{Mpc})^3$ comoving volume around the center of the halo, and post-processed UV radiative transfer (RT) using LICORICE [31]. We interpolate all gas physical properties around the halo center on a fixed 512^3 grid using the SPH kernel and smoothing length, within a $(0.156\,\mathrm{h}^{-1}\,\mathrm{Mpc})^3$ comoving volume. We then implement on top of the simulation a sub-grid model which takes into account the cooling and heating processes that set the thermal equilibrium of the neutral ISM [32, 33]. According to this model, neutral gas in the ISM is constituted by a two-phase medium in which the cold neutral medium (CNM) and the warm neutral medium (WNM) are in pressure equilibrium. The relative abundance of these two components depends on the gas metallicity, which determine the abundance of coolants, and on the flux of the Far-Ultraviolet (FUV) dissociating field in the Habing (6–13.6 eV) band (G_0), that controls the rates of photoelectric heating produced by dust grains. The value of G_0 in each computational cell is calculated:

$$G_0(\vec{r}) = \Sigma_{i=1}^{n_*} \frac{\int_{6\,\mathrm{eV}}^{13.6\,\mathrm{eV}} l_{\nu,i}\mathrm{d}\nu}{4\pi|\vec{r}-\vec{r_i}|^2}, \tag{1}$$

where n_* is the number of sources, $\vec{r_i}$ is the positions, $l_{\nu,i}$ is the monochromatic luminosity per source. We compute $l_{\nu,i}$ by using `STARBURST99` template, assuming continuos star formation, an age 10 Myr for the stellar population and setting the metallicity accordingly to the cell value. The WNM distribution closely traces regions of high ($N_H \approx 10^{22}\,\mathrm{cm}^{-2}$) total hydrogen column density that are sufficiently far from the central star forming region in order not to become ionized; cold gas lies instead only in small ($D \leq 2\,\mathrm{kpc}$) overdense clumps at the periphery of the galaxy.

3. – Atomic emission lines

For each simulated cell we calculate the line luminosities $L_i = \varepsilon_i V_{cell}$, where the emissivity of the i-th atomic species (in this case carbon and oxygen) $\varepsilon_i = \varepsilon_i(n_H, T)$ depends on the density (n_H) and the temperature (T) of the WNM/CNM. The C and O abundances are assumed to scale linearly with the metallicity Z.

In fig. 1 we show the predicted [CII] 158 μm, and [OI] 63 μm emission for the spectral resolution of our simulations ($1.0\,\mathrm{km\,s}^{-1}$), a beam resolution of 0.1 arcsec and $Z = Z_\odot$, along with the maps obtained by integrating the spectra over the full velocity range $-200 < v < 300\,\mathrm{km\,s}^{-1}$.

The [CII] spectrum contains considerable structure due to the presence of several emitting CNM clumps distributed over the entire galaxy's body ($\sim 20\,\mathrm{kpc}$). The individual sizes of the clumps are however much smaller ($< 3\,\mathrm{kpc}$). The peak of the spectrum reaches $\sim 2.5\,\mathrm{mJy}$ and it is displaced from the center of the galaxy by about $100\,\mathrm{km\,s}^{-1}$. The FWHM of the main peak is $\sim 50\,\mathrm{km\ s}^{-1}$, consistent with the marginal detection of [CII] in high-z LAEs [34].

The displacement of the main peak is due to the fact that the gas within the central kpc of our Galaxy is highly ionized by the massive stars that form there. However we point out that the sub-grid model presented here *does not* include molecular clouds and hence emission from dense photodissociation regions that are expected to be close to the sites of star formation. Hence, the spectra in fig. 1 have to be considered as a lower limits on the total emission.

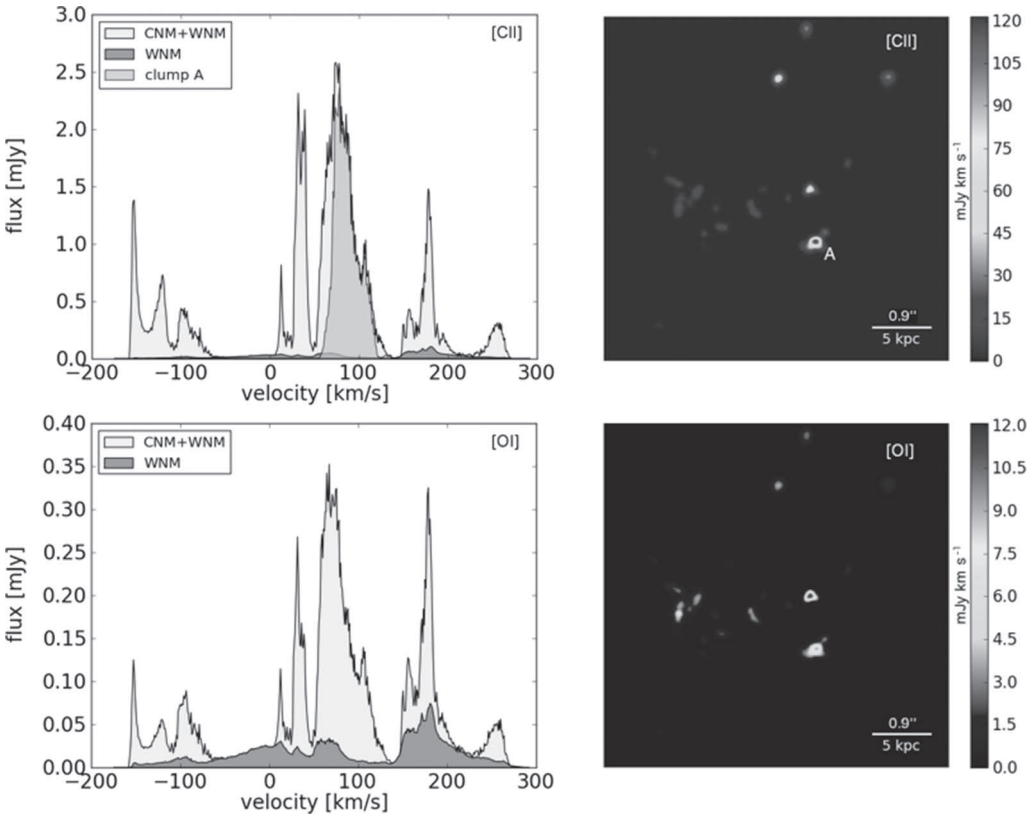

Fig. 1. – Left column: The total (CNM+WNM) and WNM only (dark gray) spectrum of [CII], and [OI] binned in 1.0 km s^{-1} channels. Right column: [CII], and [OI] maps in mJy km s^{-1} with resolution of 0.1 arcsec and integrated over the entire spectral velocity range. The contribution of clump A to the [CII] spectrum is plotted in light gray.

We find that 95% of the total [CII] flux from the diffuse gas originates from the CNM, and only 5% from the WNM. For the [CII] emission line we obtain a flux of 185 mJy km s^{-1}, integrating over ~ 500 km s^{-1}.

In fig. 1 we plot in grey the spectrum extracted by integrating over a circular area of ~ 2 kpc radius, centered on the component labeled A in the map. It dominates the peak of the [CII] spectrum (30% contribution to the total emission), with the remaining ~ 70% coming from less luminous substructures.

The [OI] spectrum has a shape similar to that of [CII] since for both emission lines we are taking into account the emission arising from the neutral phase of the ISM. In the case of [OI], 75% of the total flux arises from the CNM and 25% from the WNM. The maximum value of the [OI] flux is ~ 0.35 mJy.

We have computed FIR line intensities also for a metallicity $Z = 0.02\ Z_{\odot}$. In this case, the [CII] and [OI] intensities drop by a factor of ~ 1000 and ~ 300, respectively. While the WNM emission is $\propto Z$, at very low Z CNM is practically absent, since the lower metal content makes the CNM phase thermodynamically unfavorable.

These synthetic spectra are exquisite examples of the potential of using cosmological simulation to i) interpret upcoming data from ALMA observations and ii) to construct physically motivated observational proposal based on the model predictions.

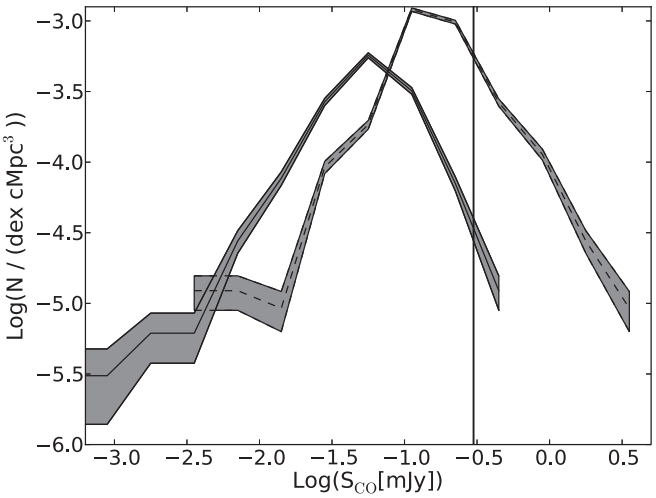

Fig. 2. – The number density of LAEs at $z \approx 5.7$ and 6.6 are shown as a function of the line integrated CO(6-5) flux using dashed and solid lines respectively; shaded regions show the poissonian errors. The vertical solid line represent the ALMA sensitivity limits for 50 antennas assuming a signal to noise ratio, $S/N = 5$, for an integration time 10 hours.

4. – Molecular emission lines

Whereas for the metal cooling lines we preferred a zoomed cosmological simulation to achieve a spatial resolution that allows to construct high-resolution spectra (see fig 1), we have also exploited calculations on large sample of simulated $z \approx 6$ galaxies to provide theoretical predictions on the luminosity function of molecular lines.

To do so, we start by using a previously developed LAE sample [35-37] (at $z =$ 5.7–6.6), where the authors combined state-of-the-art cosmological SPH simulations with a Lyα production/transmission model to successfully reproduce a large number of observational data sets. We couple the sample resulting from their analysis, with a semi-analytic model that describes the structure of the molecular clouds. The approach, proposed by [38-40], allows calculate the molecular fraction ($f_{\rm H_2}$) taking into account its formation on dust grains, its destruction by UV photons, and the shielding by [HI] in the ISM starting from few inputs: (A) the free space photon number density in the Lyman Werner band, (B) the dust absorption cross-section per hydrogen nucleus to Lyman Werner photons, (C) the number density of gas in the cold atomic medium that surrounds the molecular part of the cloud, and (D) the rate of H_2 formation on the surface of dust grains.

We defer the interested reader to [41] where we examine in details the correlations of $f_{\rm H_2}$ with the physical properties of the emitters including the SFR, the dust mass, and the amount of cold neutral gas in the ISM. The main point that we want to discuss here is that we translate the total molecular mass ($M_{\rm H_2} = f_{\rm H_2} M_{gas}$) into the CO(1-0) luminosity by adopting $\alpha = 0.8\, M_\odot\, {\rm K\,km\,s^{-1}}$. Then, by assuming Local Thermal Equilibrium, we achieve the luminosity of lowest CO rotational line observable with the ALMA arising from $z \sim 5.7$–6.6: the CO(6-5).

The main result of our calculation is shown in fig. 2 were we plot the flux function, *i.e.* the number density of LAEs as a function of the line-integrated CO flux, $S_{\rm CO}$(6-5). The use of 50 ALMA antennas with and integration time of 10 hours would allow the sampling of the high-luminosity tail of the co flux function at both the redshifts considered.

5. – Conclusions

In this paper we discussed the potential of developing physically motivated models that allows to predict the luminosity of several FIR (atomic and molecular) lines that are observable with ALMA. On the one side, we show the synergy between a zoomed RT simulation of a $z = 6.6$ galaxy and a sub-grid model developed to describe the thermodynamic equilibrium of the diffuse neutral gas whitin the galaxy ISM. This allows to construct the high resolution spectra of metal cooling lines arising from the cold and warm neutral diffuse phase of the ISM. We predict that the expected [CII] and [OI] can be used to constrain the metallicity of such galaxies.

On the other side, we briefly presented a semi-analytical physically motivated calculation that allows to build the CO(6-5) flux function at $z = 5.7 - 6.6$ from a sample of simulated LAEs. We show the capabilities of ALMA in recovering the high-luminosity tail of the flux function at both redshifts.

REFERENCES

[1] Dunlop J. S., *Observing the First Galaxies*, in *Proceedings of Astrophysics and Space Science Library*, edited by Wiklind T., Mobasher B. and Bromm V.,, *Astrophysics and Space Science Library*, Vol. **396** (2013) p. 223.
[2] Steidel C. C., Giavalisco M., Dickinson M. and Adelberger K. L., *Astron. J.*, **112** (1996) 352.
[3] Castellano M., Fontana A., Paris D., Grazian A., Pentericci L., Boutsia K., Santini P., Testa V., Dickinson M., Giavalisco M., Bouwens R., Cuby J.-G., Mannucci F., Clément B., Cristiani S., Fiore F., Gallozzi S., Giallongo E., Maiolino R., Menci N., Moorwood A., Nonino M., Renzini A., Rosati P., Salimbeni S. and Vanzella E., *Astron. Astrophys.*, **524** (2010) A28.
[4] Bouwens R. J., Illingworth G. D., Oesch P. A., Labbé I., Trenti M., van Dokkum P., Franx M., Stiavelli M., Carollo C. M., Magee D. and Gonzalez V., *Astrophys. J.*, **737** (2011) 90.
[5] McLure R. J., Dunlop J. S., de Ravel L., Cirasuolo M., Ellis R. S., Schenker M., Robertson B. E., Koekemoer A. M., Stark D. P. and Bowler R. A. A., *Mon. Not. R. Astron. Soc.*, **418** (2011) 2074.
[6] Malhotra S., Rhoads J. E., Pirzkal N., Haiman Z., Xu C., Daddi E., Yan H., Bergeron L. E., Wang J., Ferguson H. C., Gronwall C., Koekemoer A., Kuemmel M., Moustakas L. A., Panagia N., Pasquali A., Stiavelli M., Walsh J., Windhorst R. A. and di Serego Alighieri S., *Astrophys. J.*, **626** (2005) 666.
[7] Shimasaku K., Kashikawa N., Doi M., Ly C., Malkan M. A., Matsuda Y., Ouchi M., Hayashino T., Iye M., Motohara K., Murayama T., Nagao T., Ohta K., Okamura S., Sasaki T., Shioya Y. and Taniguchi Y., *Publ. Astron. Soc. Jpn.*, **58** (2006) 313.
[8] Hu E. M., Cowie L. L., Barger A. J., Capak P., Kakazu Y. and Trouille L., *Astrophys. J.*, **725** (2010) 394.
[9] Ouchi M., Shimasaku K., Furusawa H., Saito T., Yoshida M., Akiyama M., Ono Y., Yamada T., Ota K., Kashikawa N., Iye M., Kodama T., Okamura S., Simpson C. and Yoshida M., *Astrophys. J.*, **723** (2010) 869.
[10] Kennicutt R. C. and Evans N. J., *Astron. Astrophys.*, **50** (2012) 531.
[11] Stacey G. J., Geis N., Genzel R., Lugten J. B., Poglitsch A., Sternberg A. and Townes C. H., *Astrophys. J.*, **373** (1991) 423.
[12] Ferkinhoff C., Brisbin D., Nikola T., Pardhley S. C., Stacey G. J., Phillips T. G., Falgarone E., Benford D. J., Staguhn J. G. and Tucker C. E., *Astrophys. J.*, **740** (2011) L29.

[13] Nagao T., Maiolino R., De Breuck C., Caselli P., Hatsukade B. and Saigo K., *Astron. Astrophys.*, **542** (2012) L34.
[14] Decarli R., Walter F., Neri R., Bertoldi F., Carlli C., Cox P., Kneib J. P., Lestrade J. F., Maiolino R., Omont A., Richard J., Riechers D., Thanjavur K. and Weiss A., *Astrophys. J.*, **752** (2012) 2.
[15] Combes F., Rex M., Rawle T. D., Egami E., Boone F., Smail I., Richard J., Ivison R. J., Gurwell M., Casey C. M., Omont A., Berciano Alba A., Dessauges-Zavadsky M., Edge A. C., Fazio G. G., Kneib J.-P., Okabe N., Pelló R., Pérez-González P. G., Schaerer D., Smith G. P., Swinbank A. M. and van der Werf P., *Astron. Astrophys.*, **538** (2012) L4.
[16] Strum E., Verma A., Graciá-Carpio J., Hailey-Dunsheath S., Contursi A., Fischer J., González-Alfonso E., Poglitsch A., Sternberg A., Genzel R., Lutz D., Tacconi L., Christopher N. and de Jong J., *Astron. Astrophys.*, **518** (2010) L36.
[17] Maiolino R., Cox P., Caselli P., Beelen A., Bertoldi F., Carilli C. L., Kaufman M. J., Menten K. M., Nagao T., Omont A., Weiss A., Walmsley C. M. and Walter F., *Astron. Astrophys.*, **440** (2005) L51.
[18] Cox P., Krips M., Neri R., Omont A., Güsten R., Menten K. M., Wyrowski F., Weiss A., Beelen A., Gurwell M. A., Dannerbauer H., Ivison R. J., Negrello M., Aretxaga I., Hughes D. H., Auld R., Baes M., Blundell R., Buttiglione S., Cava A., Cooray A., Dariush A., Dunne L., Dye S., Eales S. A., Frayer D., Fritz J., Gavazzi R., Hopwood R., Ibar E., Jarvis M., Maddox S., Michałowski M., Pascale E., Pohlen M., Rigby E., Smith D. J. B., Swinbank A. M., Temi P., Valtchanov I., van der Werf P. and de Zotti G., *Astrophys. J.*, **740** (2011) 63.
[19] De Breuck C., Maiolino R., Caselli P., Coppin K., Hailey-Dunsheath S. and Nagao T., *Astron. Astrophys.*, **530** (2011) L8.
[20] Gallerani S., Neri R., Maiolino R., Martín S., De Breuck C., Walter F., Caselli P., Krips M., Meneghetti M., Nagao T., Wagg J. and Walmsley M., *Astron. Astrophys.*, **543** (2012) A114.
[21] Venemans B. P., McMahon R. G., Walter F., Decarli R., Cox P., Neri R., Hewett P., Mortlock D. J., Simpson C. and Warren S. J., *Astrophys. J.*, **751** (2012) L25.
[22] Carilli C. L., Riechers D., Walter F., Maiolino R., Wagg J., Lentati L., McMahon R. and Wolfe A., *Astrophys. J.*, **763** (2013) 120.
[23] Carniani S., Marconi A., Biggs A., Cresci G., Cupani G., D'Odorico V., Humphreys E., Maiolino R., Mannucci F., Molaro P., Nagao T., Testi L. and Zwaan M. A., *Astron. Astrophys.*, **559** (2013) A29.
[24] Williams R. J., Wagg J., Maiolino R., Foster C., Aravena M., Wiklind T., Carilli C. L., McMahon R. G., Riechers D. and Walter F., *Mon. Not. R. Astron. Soc.*, **439** (2014) 2096.
[25] Riechers D. A., Carilli C. L., Capak P. L., Scoville N. Z., Smolčić V., Schinnerer E., Yun M., Cox P., Bertoldi F., Karim A. and Yan L., *Astrophys. J.*, **796** (2014) 84.
[26] Ouchi M., Ellis R., Ono Y., Nakanishi K., Kohno K., Momose R., Kurono Y., Ashby M. L. N., Shimasaku K., Willner S. P., Fazio G. G., Tamura Y. and Iono D., *Astrophys. J.*, **778** (2013) 102.
[27] Ota K., Walter F., Ohta K., Hatsukade B., Carilli C. L., da Cunha E., González-López J., Decarli R., Hodge J. A., Nagai H., Egami E., Jiang L., Iye M., Kashikawa N., Riechers D. A., Bertoldi F., Cox P., Neri R. and Weiss A., *Astrophys. J.*, **792** (2014) 34.
[28] Schaerer D., Boone F., Zamojski M., Staguhn J., Dessauges-Zavadsky M., Finkelstein S. and Combes F., *Astron. Astrophys.*, **574** (2015) A19.
[29] Vallini L., Gallerani S., Ferrara A. and Baek S., *Mon. Not. R. Astron. Soc.*, **433** (2013) 1567.
[30] Springel V., *Mon. Not. R. Astron. Soc.*, **364** (2005) 1105.

[31] Baek S., Di Matteo P., Semelin B., Combes F. and Revaz Y., *Astron. Astrophys.*, **495** (2009) 389.
[32] Wolfire M. G., Hollenbach D., McKee C. F., Tielens A. G. G. M. and Bakes E. L. O., *Astrophys. J.*, **443** (1995) 152.
[33] Wolfire M. G., McKee C. F., Hollenbach D. and Tielens A. G. G. M., *Astrophys. J.*, **587** (2003) 278.
[34] Carilli C. and Walter A., arxiv (2013).
[35] Dayal P., Ferrara A. and Gallerani S., *Mon. Not. R. Astron. Soc.*, **389** (2008) 1683.
[36] Dayal P., Ferrara A., Saro A., Salvaterra R., Borgani S. and Tornatore L., *Mon. Not. R. Astron. Soc.*, **400** (2009) 2000.
[37] Dayal P., Ferrara A. and Saro A., *Mon. Not. R. Astron. Soc.*, **402** (2010) 1449.
[38] Krumholz M. R., McKee C. F. and Tumlinson J., *Astrophys. J.*, **689** (2008) 865.
[39] Krumholz M. R., McKee C. F. and Tumlinson J., *Astrophys. J.*, **693** (2009) 216.
[40] McKee C. F. and Krumholz M. R., *Astrophys. J.*, **709** (2010) 308.
[41] Vallini L., Dayal P. and Ferrara A., *Mon. Not. R. Astron. Soc.*, **421** (2012) 3266.